

## Vortex String Formation in a 3D U(1) Temperature Quench

Nuno D. Antunes,<sup>1</sup> Luís M. A. Bettencourt,<sup>2</sup> and Wojciech H. Zurek<sup>2</sup>

<sup>1</sup>*Département de Physique Théorique, Université de Genève, 24 quai E. Ansermet, CH 1211, Genève 4, Switzerland*

<sup>2</sup>*Theoretical Division MS B288, Los Alamos National Laboratory, Los Alamos, New Mexico 87545*  
(Received 23 November 1998)

We report the first large scale numerical study of the dynamics of a second order phase transition caused by a gradual decrease of temperature in a U(1)  $\lambda\phi^4$  theory in three spatial dimensions. We present a detailed account of the dynamics of the fields and focus on vortex string formation as a function of the quench rate. The results are found in good agreement with the theory of defect formation proposed by Kibble and Zurek. [S0031-9007(99)08817-1]

PACS numbers: 11.30.Qc, 05.70.Fh, 11.27.+d, 98.80.Cq

Topological defects are of fundamental importance to the (thermo)dynamics of phase transitions in some of the most fascinating materials in the laboratory—e.g., superfluids, type II superconductors, liquid crystals—and presumably also to symmetry breaking phase transitions in the early universe [1]. When present at low energies they constitute the last traces of disorder inherited from high temperatures and thus determine the nonequilibrium evolution of many systems.

The theory of defect formation combines the realization, due to Kibble [2], of the paramount role of causality, with the calculation, due to one of us [3], of the actual size of the causally independent domains in a second order phase transition. Experiments in liquid crystals [4] and in <sup>3</sup>He [5] lend support to the resulting theory of the dynamics of second order phase transitions. The evidence from <sup>4</sup>He experiments [6] is more ambiguous while superconductors and Bose-Einstein condensates may offer exciting future possibilities [7].

Laboratory experiments were thus far unable to test the key theoretical prediction—the scaling of the initial density of defects with the rate at which the phase transition takes place [3]. Numerical studies of defect formation as a function of a quench rate carried out until now were limited to 1D and 2D systems [8], where they have confirmed the scalings predicted by the theory. Moreover, they have focused on transitions induced by the explicit change of the mass term in the potential which governs dynamics of the order parameter field  $\langle\phi\rangle$ , while the temperature  $T$  of the heat bath to which  $\phi$  is coupled was kept constant and relatively small. This simplification is not necessarily unrealistic—phase transitions in <sup>4</sup>He can be induced without significant changes in temperature, purely by changing pressure. However such “pressure quenches” are far less common than temperature quenches, and temperatures are rarely small. Moreover, the analytic approach to the pressure quench problem seems to be within reach, although only in the limit of very small temperatures. Even in this limiting case unanimous conclusion has not been reached [9–11], further obviating the need to study quenches numerically.

Indeed, the emerging understanding of the defect production could be called into question on the grounds that the present estimates completely ignore the inevitable Ginzburg regime. There, just below  $T_c$ , fluctuations can rearrange large spatial regions, which could destroy protodefects produced by freeze-out [3], or create them at densities set by the Ginzburg length, as it was originally suggested [2] and is still occasionally argued [9].

In this Letter, we perform the first large-scale numerical studies of a gradual temperature quench in 3D U(1) symmetric  $\lambda\phi^4$  [12]. This is the familiar Ginzburg-Landau model for the free energy of a neutral system (e.g., <sup>4</sup>He) which as is well known displays a true second order phase transition in 3D, with the establishment of long range order at low temperatures. This implies, in particular, contrary to the case of lower dimensions, that no defects (vortex strings) can exist in equilibrium at sufficiently low temperatures in any causally connected volume [13].

In order to implement the temperature quench, we evolve the fields according to

$$(\partial_t^2 - \nabla^2)\phi_i - m^2\phi_i + \lambda\phi_i(\phi_i^2 + \phi_j^2) + n\dot{\phi}_i = \Gamma_i, \quad (1)$$

where  $i, j \in \{1, 2\}$  and  $i \neq j$  in Eq. (1).  $\Gamma_i(x)$  is the Gaussian noise characterized by

$$\langle\Gamma_i(x)\rangle = 0, \quad \langle\Gamma_i(x)\Gamma_j(x')\rangle = 2\eta T(t)\delta_{ij}\delta(x - x'), \quad (2)$$

where  $x, x'$  denote space-time coordinates. We allow the fields to thermalize above the transition and proceed to quench the system by changing the noise temperature as

$$T(t) = T_c - T_0 \frac{t}{t_Q}. \quad (3)$$

The time  $t_Q$  controls the rate of the quench. For  $t > \frac{T_c}{T_0}t_Q$ ,  $T = 0$ . In the numerical evolution we take the grid spacing  $\Delta x = 0.5$  and  $\Delta t = 0.02$ . All results shown are for computational domains of size  $N^3$ , with  $N = 128$ – $160$  and  $\eta = 1$ . Strings are detected by integer windings of the field phases around lattice plaquettes.

Vortices hence found are connected by enforcing flux conservation on each unit volume [13]. As a result of boundary conditions all strings are closed. Above  $T_c$ , and immediately below, strings are little more than nonperturbative field fluctuations. Below  $T_c$ , they gradually acquire stability and can be regarded as either vortex lines or cosmic strings.

Another useful quantity is the kinetic temperature,  $T_K$ , defined as the average kinetic energy per degree of freedom. In equilibrium the canonical momentum distribution is purely Gaussian and  $\langle |\pi(x)|^2 \rangle d^D x = 2T$ . We generalize this for situations away from equilibrium as

$$\langle |\pi(x, t)|^2 \rangle d^D x \equiv 2T_K(t). \quad (4)$$

All temperature quenches are started at  $T_0 = 1.91T_c$ . Even though the choice of initial (high) temperature is somewhat arbitrary, it is important that it is sufficiently high that the length density in long strings in each computational domain is substantial [13].

In the immediate vicinity of  $T_c$  for a system undergoing a second order phase transition, the dynamics of  $\phi$  are subject to critical slowing down. This leads to the estimate of the expected density of defects through an argument [3], which we briefly reproduce below. For the dynamics of Eqs. (1) and (2) in the overdamped regime where the first time derivative dominates, the characteristic time scale  $\tau$  over which the order parameter can react is given by

$$\tau_\phi \approx \frac{\eta}{m^2 |\epsilon|^{\nu z}}, \quad (5)$$

where  $\nu$  and  $z$  are universal critical exponents, and the relative temperature  $\epsilon = \frac{T}{T_c} - 1 = \frac{t}{\tau_Q} \equiv \frac{t}{t_Q} \frac{T_0}{T_c}$ . The quench time scale  $\tau_Q$  is a rescaling of  $t_Q$ ,  $\tau_Q = \frac{T_c}{T_0} t_Q$ .

This overdamped scenario, valid when  $\eta^3 \tau_Q > 1$  [8], is presumably more relevant for condensed matter applications and will be the focus of the present Letter. Cosmological order parameters may in contrast be underdamped—or in reality redshifted [1], corresponding to a different dynamics than that of Eqs. (1) and (2).

The characteristic time scale of variation of  $\epsilon$  is  $\frac{\epsilon}{\dot{\epsilon}} = t$ . We expect the system to be able to readjust to the new equilibrium as long as the relaxation time is smaller than  $t$ . Hence, outside the time interval  $[-\hat{t}, \hat{t}]$  defined by the equation  $\tau(\epsilon(\hat{t})) = \hat{t}$ , the evolution of  $\phi$  is approximately adiabatic, and physical quantities associated with large length scales will approximately follow their (critical) equilibrium values. The time

$$\begin{aligned} \hat{t}_\phi &= \pm \left[ \frac{\eta}{m^2} (\tau_Q)^{\nu z} \right]^{1/(1+\nu z)}; \\ \hat{\epsilon}_\phi &= \pm \left( \frac{\eta}{m^2} \frac{1}{\tau_Q} \right)^{1/(1+\nu z)} \end{aligned} \quad (6)$$

marks the borders between adiabatic and impulse stages of evolution of  $\phi$ . In particular, the correlation length  $\xi$  associated with the connected two-point function above the

transition will cease to increase as  $\xi = \xi_0 m_0 / |\epsilon|^\nu$  once the adiabatic-impulse boundary at  $t' = -\hat{t}$  is reached.

We expect, then, that the characteristic length scale over which  $\phi$  is ordered already in the course of the transition will be the correlation length at freeze-out  $\hat{\xi} = 1/\hat{\epsilon}^\nu$ ,

$$\hat{\xi}_\phi = \left( \frac{m^2}{\eta} \tau_Q \right)^{\nu/(1+\nu z)}. \quad (7)$$

On length scales smaller than  $\hat{\xi}$  the effect of criticality on the field dynamics is negligible. The initial density of vortex lines is then expected to scale with  $\tau_Q$  as

$$n_\phi = \frac{1}{(f_\phi \hat{\xi}_\phi)^2} = \frac{1}{f_\phi^2} \left( \frac{m^2}{\eta} \tau_Q \right)^{-\alpha}, \quad (8)$$

where  $f \sim O(1)$  is a dimensionless factor, parametrizing our ignorance about the exact relation between domain size and defect densities, and  $\alpha = -\frac{2\nu}{1+\nu z}$ . Lattice measurements and renormalization group analysis yield  $\nu = 0.6705$  and  $z = 2.03$  for the very overdamped case when the second time derivative in Eqs. (1) and (2) is completely negligible. With  $\eta = 1$  this is not truly the case. We expect  $1 \leq z \leq 2.03$ , implying  $0.568 \leq \alpha \leq 0.8$ , where the lower and upper limits refer to the underdamped case, respectively. This is different from mean-field exponents,  $\nu = 1/2$  and  $z = 2$ , implying  $\alpha_{MF} = 0.5$ .

In a temperature quench, the system is evolved from an initial state at genuinely high temperature, with a bare negative mass squared. As a result the physical mass squared,  $m_{ph}^2$ , which takes into account the self-energy generated by the high-temperature field fluctuations, is positive and potentially large. The temperature quench proceeds by the decrease of the external bath temperature at a rate given by  $\tau_Q$ , according to Eq. (3). Initially, the system locally rethermalizes to the new lower temperature. Close to the critical point, the physical mass squared approximately vanishes leading to the critical slowing down of the field response over large spatial scales. This freezes the dynamics of the order parameter: It can no longer react to the systematic changes of thermodynamic or dynamical parameters, although slow drift under the combined influence of noise and damping continues unabated, even in the large scale structure, including long strings. Critical slowing down has little effect over the small scale dynamics ( $k^2 \gg m_{ph}^2$ ), which accompanies the externally imposed change of bath temperature. In this manner, critical slowing down sows the seeds for the out-of-equilibrium dynamics to follow. Figure 1a shows the equilibrium string densities as a function of  $T_K$ , and quench trajectories for several values of  $\tau_Q$ . In 3D,  $T_K$  is dominated by small scales and generally follows faithfully the external bath  $T$  variation.

As predicted by the theory, all quenched string densities follow the equilibrium trajectory at high temperatures but start deviating just above the critical point, due to critical slowing down. The magnitude of the effect is

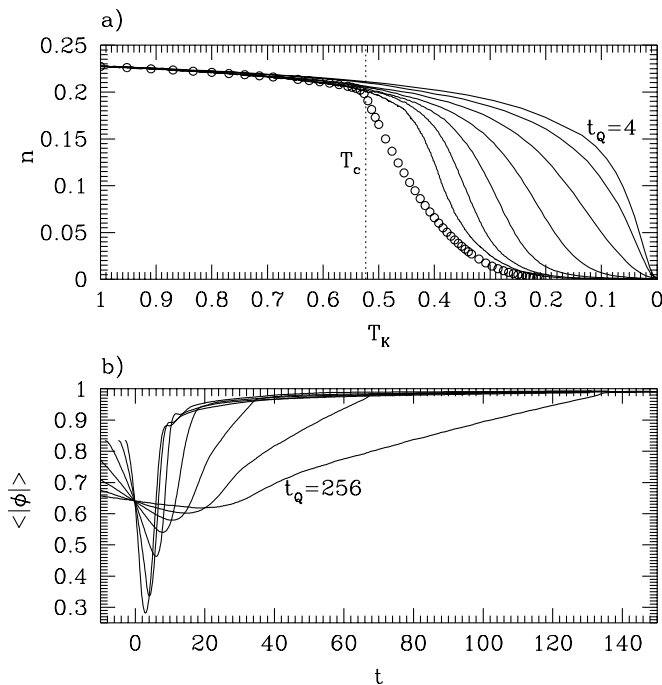


FIG. 1. (a) The evolution of the total string density per plaquette  $n$  with  $T_K$ .  $\circ$  denote thermal equilibrium densities. (b)  $\langle |\phi| \rangle$  vs  $t$ . Solid lines denote quench trajectories for  $t_Q = 4, 8, 16, 32, 64, 128, 256$ .

small and difficult to measure. After falling out of equilibrium the string densities do not freeze, but rather decay slowly while the temperature drops over a period of time. This decrease is due mostly to the decay of small scale structure in long strings and of small loops. For faster quenches this regime persists to much lower  $T_K$ . Figure 1a clearly shows the hierarchy of string densities for different  $\tau_Q$ 's, at each given  $T_K$ .

Figure 1b shows the evolution of the order parameter amplitude  $\langle |\phi| \rangle$ . The persistent cooling of small scale fluctuations eventually leads to a negative  $m_{\text{ph}}^2$  which in turn triggers instabilities in the long wavelength modes. As these modes grow (quasiexponentially) the U(1) symmetry is spontaneously broken, coarsening the original field configuration. These instabilities are reminiscent of those in pressure quenches [8–11]. However, here their generation through a negative mass squared is explicitly created by the delay in the field's response, rather than externally. The onset of instabilities defines in turn  $+\hat{t}$ , which we read off from the minima of Fig. 1b. Figure 2a shows the dependence of  $\hat{t}$  on  $\tau_Q$ . We can independently confirm the theoretical scaling laws (Fig. 2b) by examining the  $\tau_Q$  dependence of  $\hat{\epsilon}$ , computed as the ratio of  $T_K$  and  $T_c$  at the minimum of  $\langle |\phi| \rangle$ .

Together the results of Fig. 2 confirm the theoretical scaling and determine  $\nu z = 0.82$ . We note, however, that data corresponding to the fastest quenches appears to asymptote to  $|\hat{\epsilon}| = 1$  (and, thus, ceases following the predicted power law). This is easy to understand [8]:  $\hat{\epsilon}$ , extracted from the data, is the absolute value of the relative temperature at the instant when the dynamics is

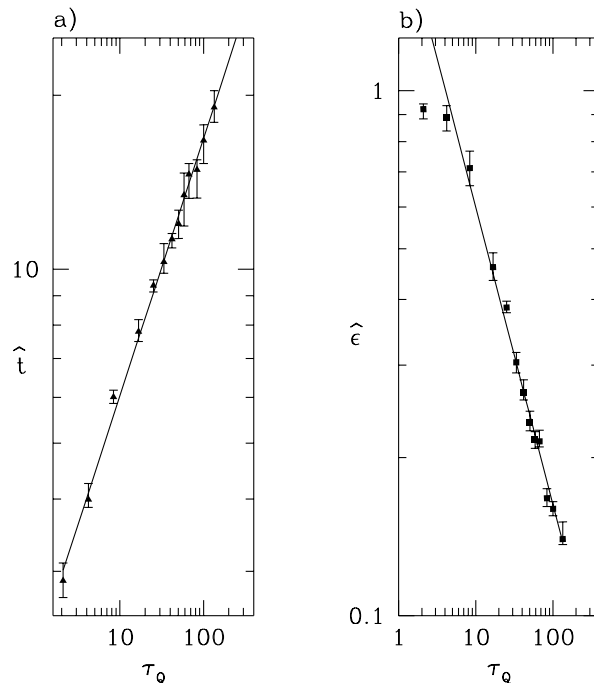


FIG. 2. (a) The freeze-out time  $\hat{t}$  as a function of the quench time scale  $\tau_Q$ . (b) The relative kinetic temperature at  $\hat{t}$ ,  $|\hat{\epsilon}| = |\frac{T_K(\hat{t})}{T_c} - 1|$ . Slopes of the two lines are  $0.445 \pm 0.05$  and  $-0.565 \pm 0.016$ , respectively, which compares favorably with those theoretically predicted of 0.5. Points corresponding to  $\tau_Q \leq 8$  exhibit saturation, and were ignored in the fitting.

restarted. But  $\epsilon = T_K/T_c - 1$ , by definition, cannot fall to less than  $-1$  (which happens when  $T_K = 0$ ). Hence, when in very fast quenches the evolution of  $\phi$  restarts only at  $\hat{t} \geq \tau_Q$ ,  $T_c \gg T_K(\tau_Q) \approx 0$ , and the values of  $|\hat{\epsilon}|$  pile up asymptotically near  $1^-$ , causing saturation.

At  $t = \hat{t}$  many small scale fluctuations still persist in the system obscuring the results in terms of string densities. It is the subsequent out-of-equilibrium evolution of the fields, leading to spontaneous symmetry breaking and ordering, that reveals the string densities formed at the quench. While the large spatial scales ( $k^2 \approx 0$ ) are unstable and the corresponding modes grow towards  $|\phi| = 1$ , the small spatial scales ( $k^2 \gg m_{\text{ph}}^2$ ) are dissipated away. This leads to the emergence of the field configuration created by the critical dynamics on large spatial scales, and allows the surviving vortex strings to form, i.e., to acquire their low energy character of topological defects. These densities, as a function of  $\tau_Q$ , are shown in Fig. 3. As a criterion to the completion of the transition, we measured  $n$  at  $t$  such that  $\langle |\phi| \rangle = 0.9, 0.925, 0.95, 0.975$ . Apart from the cases of saturation, the density of strings formed follows the theoretical predictions quite satisfactorily, for all choices of  $\langle |\phi| \rangle$ . The values of  $f_\phi = O(10)$  are similar to 1D and 2D estimates [8], and may be sufficient to explain the nonappearance of vortex lines in the recent  $^4\text{He}$  experiment [6].

Finally, it is interesting to investigate what kind of strings are formed. At  $T$  above  $T_c$ , the “ephemeral string” length distribution approaches a Brownian form

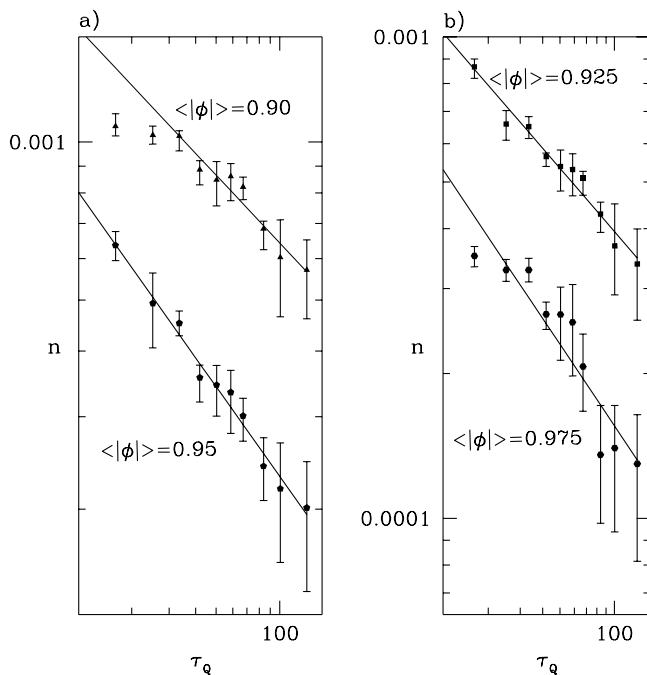


FIG. 3. The string densities measured at  $\langle |\phi| \rangle = 0.9, 0.925, 0.95, 0.975$ . The fits are to Eq. (8), for  $\tau_Q \geq 32$ , with  $\alpha = 0.4296 \pm 0.043, 0.4378 \pm 0.0289, 0.5692 \pm 0.0256, 0.5600 \pm 0.0797$ , and  $f_\phi = 11.11, 13.99, 12.29, 15.34$ , respectively. The average  $\bar{\alpha} = 0.4982 \pm 0.079$  and  $\bar{f}_\phi = 13.18 \pm 1.78$ .

[13]. Long random-walk-like strings of zeros of  $\phi$  coexist in equilibrium with a sea of smaller strongly self-correlated loops. As the quench proceeds small scales are dissipated first. Nevertheless, the presence of noise and absence of the restoring dynamics implies that until  $t \simeq +\hat{t}$  a sizable population of small loops can persist. Subsequently the system is dissipated further, the symmetry is spontaneously broken, and the fields order starting from the small scales. The result is that, by the time  $\langle |\phi| \rangle$  has come near its equilibrium low-temperature value, only long strings, imprinted by the critical dynamics on largest length scales, survive, stripped of most of their small scale structure. This evolution is shown in Fig. 4.

Our numerical analysis lends strong support to the general picture of dynamical evolution of  $\langle |\phi| \rangle$  in a second order phase transition, proposed some time ago [3], and partially confirmed by experiments [5] and by simulation of pressure quenches in low dimensional systems [8]. The key new aspects of this investigation are (i) its 3D character, which has allowed us to (ii) study an until now numerically unexplored temperature quench. In the present range of parameters the Ginzburg regime appeared to play no discernible role. We are currently investigating its effects on the decay of individual strings.

We thank A. Gill, T. Kibble, P. Laguna, R. Rivers, and A. Yates for useful discussions. Numerical work was done on the T-division/CNLS Avalon Beowulf cluster,

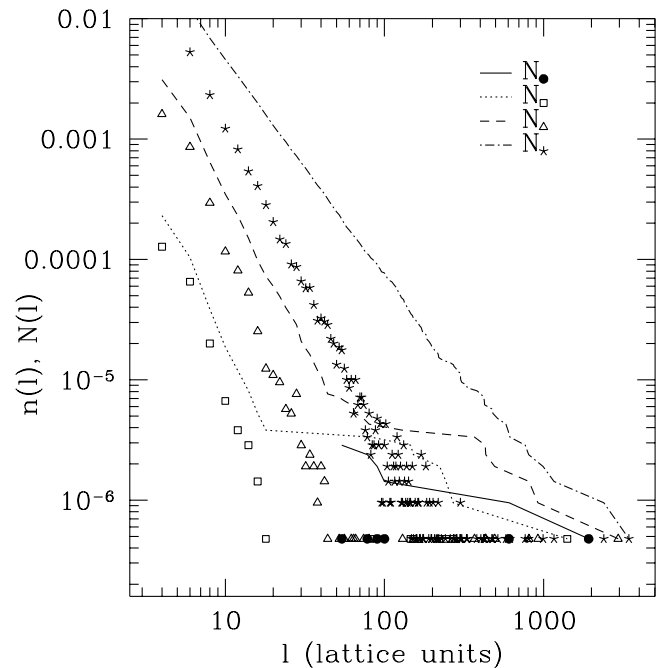


FIG. 4. String length  $l$  distributions ( $n dl$  vs  $l$ ) taken between  $+\hat{t}$  and the “time of formation” ( $\langle |\phi| \rangle = 0.95$ ), for  $\tau_Q = 64$ . Data sets denoted by  $(*, \Delta, \square, \bullet)$  correspond to increasingly later times. Lines show the integral distributions, e.g.,  $N_*(l) = \int_l^\infty n_*(l') dl'$ .

LANL, and supported by DOE, Contract No. W-7405-ENG-36.

- [1] A. Vilenkin and E.P.S. Shellard, *Cosmic Strings and Other Topological Defects* (Cambridge University, Cambridge, England, 1994).
- [2] T.W.B. Kibble, *J. Phys. A* **9**, 1387 (1976).
- [3] W.H. Zurek, *Nature (London)* **317**, 505 (1985); *Acta Phys. Pol. B* **24**, 1301 (1993); *Phys. Rep.* **276**, 177 (1996).
- [4] I. Chuang *et al.*, *Science* **251**, 1336 (1991); M.J. Bowick *et al.*, *ibid.* **263**, 943 (1994).
- [5] C. Bäuerle *et al.*, *Nature (London)* **382**, 332 (1996); V.M.H. Ruutu *et al.*, *Nature (London)* **382**, 334 (1996); V.M.H. Ruutu *et al.*, *Phys. Rev. Lett.* **80**, 1465 (1998); see also V.B. Eltsov, M. Krusius, and G.E. Volovik, cond-mat/9809125.
- [6] P.C. Hendry *et al.*, *Nature (London)* **368**, 315 (1994); M.E. Dodd *et al.*, *Phys. Rev. Lett.* **81**, 3703 (1998).
- [7] J.R. Anglin and W.H. Zurek, quant-ph/9804035.
- [8] P. Laguna and W.H. Zurek, *Phys. Rev. Lett.* **78**, 2519 (1997); *Phys. Rev. D* **58**, 085021 (1998); A. Yates and W.H. Zurek, *Phys. Rev. Lett.* **80**, 5477 (1998).
- [9] G. Karra and R.J. Rivers, *Phys. Rev. Lett.* **81**, 3707 (1998).
- [10] J. Dziarmaga, *Phys. Rev. Lett.* **81**, 1551 (1998).
- [11] G.D. Lythe, *An. Fis.* **4**, 55 (1998).
- [12] See also M. Mondello and N. Goldenfeld [*Phys. Rev. A* **45**, 657 (1992)] for a 3D study of phase ordering kinetics.
- [13] N.D. Antunes, L.M.A. Bettencourt, and M. Hindmarsh, *Phys. Rev. Lett.* **80**, 908 (1998); N.D. Antunes and L.M.A. Bettencourt, *ibid.* **81**, 3083 (1998).